Comparative analysis of freeze drying and spray drying methods for encapsulation of chlorophyll with maltodextrin and whey protein isolate

Shahrbanoo Amadi Ledri [a], Jafar M. Milani [a,*], Seyed-Ahmad Shahidi [b], Abdolkhaleg Golkar [c]

[a] Department of Food Science and Technology, Faculty of Agricultural Engineering, Sari Agricultural Sciences and Natural Resources University, P.O. Box: 578, Sari 4818168984, Iran
[b] Department of Food Science and Technology, Ayatollah Amoli Branch, Islamic Azad University, Amol, Iran
[c] Freer Flavour and Colour Company, Isfahan 8415683111, Iran

A B S T R A C T

Chlorophyll (Chl) is a healthy green pigment that is very unstable. So, chlorophyll microcapsules were fabricated using maltodextrin and whey protein isolate as carriers and freeze-drying (FD) and spray-drying (SD) as encapsulation methods. The microcapsules obtained by the freeze-drying method (FDM) had smaller particle sizes (1.087–0.165 μm) and higher ζ-potential (−10.6 to −18.3 mV) than the spray-drying method (SDM) (3.420–0.285 μm) and (−9.5 to −10.7 mV) respectively. FTIR, XRD, and DSC studies showed that the inclusion of Chl within microcapsules and FDM had a higher melting point (150.12 °C) than SDM (125.03 °C) and Chl (115.66 °C). FD was more effective in protecting Chl from changes in pH (pH 2 to 8, Chl retention; 49.67 %–91.28 %) and light (Chl retention; 38.12 %) than SD. Therefore, due to preserving Chl and increasing its stability, FDM could be a promising approach to use as a natural food colourant.

1. Introduction

Food colourants are a group of additives that are prepared naturally or artificially and are considered important and influential factors in the appearance and marketability of food (Hu et al., 2022). Natural bioactive compounds help develop health-oriented functional food products with proper quality factors. Chlorophyll (Chl) is a bioactive compound and natural green pigment in photosynthetic organisms like algaes and plants. being consumed as part of vegetables and fruits, it plays a main role in the human diet (Hanafy et al., 2021; Pemmaraju et al., 2018). Nevertheless, its instability against processing conditions makes the fail to act as a sufficient colouring agent (Roca et al., 2016). It is sensitive to acidic pH and high temperatures. For example, its exposure to acidic media results in the replacement of its magnesium by two hydrogen atoms, leading to the production of pheophytin, brown. Following is the classification of the most frequently utilized green protection strategies: i) Ion replacement: using metal ions, like Cu^{2+} and Zn^{2+}, ii) Alkalization: Alkalizers increase the products' pH and improve Chl stability and iii) Inhibiting enzyme activity (Li et al., 2022).

The increase in the storage time leads to a gradual decrease in the protective effect of alkalinization. Besides, the excessive use of copper ion, as a heavy metal, is harmful to the human body. however, the use of

zinc ions for ion replacement is a helpful alternative (Chasapis et al., 2020). Not only do zinc ions improve chlorophyll's tolerance to heat, acid, etc., but they also affect beneficially on human health with moderate intake via strengthening the immune system (Ong et al., 2014). The bearable upper limit of intake is 40 mg/day in adults. The protection of these natural bioactive compounds from degradation during various processing and storage conditions is done via microencapsulation (Mehta et al., 2022). It is a new immobilization approach for various active compounds, either gas, solids, or liquid in small capsules, enabling the release of the content at controlled and specified conditions (Domínguez et al., 2021). It is of critical importance to select appropriate wall material for a particular core material in encapsulation. Among all wall materials, proteins are the most advantageous given their high nutritional value and their easy digestion by the human gastrointestinal tract (Chen et al., 2006). As a byproduct of the dairy industry, whey protein isolate (WPI) is produced vastly worldwide. It has proper functional and nutritional features, capable of successful entrapping of hydrophobic compounds (Abbasi et al., 2014).

Maltodextrins (MD) are considered hydrolysed starches from corn, potato and wheat. MD differ based on their degrees of dextrose equivalence. The MD with dextrose equivalence from 10 to 20 is vastly utilized thanks to its high-water solubility, low viscosity, flavourlessness,

---

easy biodegradability, formation of encapsulated products with excellent oxidation stability and capability of providing an economical (Apintanapong & Noomhorm, 2003). yet, it suffers from some restrictions, the most important of which are its low emulsifying capacity and marginal retention of volatiles (Šturm et al., 2019). Therefore, it is commonly mixed with other wall materials to form stable emulsions, like whey protein (Kang et al., 2019).

The most commonly used methods of encapsulation are Freeze-drying (FD) and spray-drying (SD). Notwithstanding an extremely long dehydration period, FD is among the most helpful processes for drying thermosensitive substances, but the process is relatively slow and expensive. Yet, SD is utilized more vastly for encapsulation in the food industry, owing to its lower cost and flexibility. It is commonly utilized in preparing dry and stable food additives and flavours.

Some researchers have endeavoured to synthesize microcapsules for Chl (Agarry et al., 2023; Agarry, Wang, Cai, Wu, et al., 2022; Hsiao et al., 2020; Kang et al., 2019; Kang et al., 2018; Kurniasih et al., 2018; Raei et al., 2017; Zhang et al., 2019; Zhang et al., 2020).

However, to the best of our knowledge, there are no reports on the simultaneous use of MD and WPI as a wall and comparison of two FD and SD methods. In this study, encapsulation was used to increase the stability of chlorophyll extracted from *Ulva intestinalis* algae. WPI and MD were used as wall materials and SD and FD were used as encapsulation methods. To obtain the composition ratio of wall and core materials, Design Expert software was used. In this plan, MD (X_1), WPI (X_2), and Chl (X_3) were investigated as independent variables, and encapsulation efficiency and chlorophyll content of microcapsules as responses. Finally, employing the optimization method, the microcapsules with the highest efficiency and chlorophyll content in the two methods (FD & SD) were selected. Eventually, the microcapsules were characterized using FT-IR spectroscopy, differential scanning calorimetry (DSC), and X-ray diffraction (XRD), and finally, the evaluation of particle size, colour, and the storage stability of these microcapsules at different conditions (temperatures, light, pH) was carried out.

2. Material and methods

2.1. Materials

Ulva intestinalis macroalgae used in this study were collected from the shores of the Caspian Sea. Whey protein isolate (Hilmar Co., America), Maltodextrin (DE 17–20, Sigma Aldrich), Tween 80 (Merck Co., Germany), acetone (Asia Research Co., Iran) and ethanol (Khorasan Distillation Co., Iran) were purchased. Other chemicals utilized in the study were of analytical grade.

2.2. Chlorophyll extraction

The fresh seaweed samples were first washed with seawater and then with fresh water to remove sand and impurities. Then, the seaweed was chopped finely to decrease its size. To extract the pigment, acetone 90 % was used as a solvent. After mixing 25 mg of the moist sample with 10 mL of the solvent, it was placed in a shaking incubator at a temperature of 20 °C, away from light, for 4–6 hr (Sasadara et al., 2021). After that, the extract was filtered and centrifuged at 5000 rpm for 10 min. A rotary evaporator (IKA, RV10) under vacuum at 35 °C was utilized to concentrate the extracted Chl and separate the solvent. Finally, the concentrated extract was stored in screw-top glass bottles in a freezer at a temperature of −18 °C.

2.3. Preparation of chlorophyll microcapsules (Chl-Ms)

After dissolving WPI in distilled water, it was stirred for 12 hr using a magnetic stirrer until it swelled completely. MD is dissolved in distilled water, heated at 65 °C, and stirred for 30 min. After that, WPI and MD were mixed in the proportions defined by Design Expert software (Free ver.) as a mixture of encapsulating agents and stirred for 40 min to obtain the aqueous phase (Table S1). Then, they were maintained overnight in the refrigerator at 4 ± 0.5 °C to permit the polymer molecules to hydrate completely. Flowingly, the addition of 1.5 % (w/v) of Tween 80 to the solutions of hydrated wall materials was done, followed by its complete dissolution by vigorous stirring at ambient temperature. After adding the pure Chl solution (90.71 μg/mL) to the wall material solution as the core material in defined proportions, it was homogenized at a speed of 1000 rad/min for 5 min.

To dry the microcapsules, a spray dryer, and freeze dryer were used. FD started with the freezing process by freezing the emulsions at −18 °C for 12 hr. Glass containers attached to the freeze-dryer unit were used to store the frozen samples. The FD process was carried out utilizing a laboratory desktop freeze-dryer (ZiRBUS, VaCo 5, Germany) with a condenser at −50 °C and a vacuum of 0.1 mbar for 48 hr. Spray dryer (Dorsa Behsaz Co., D26, Iran) with an outlet air temperature of 110 °C and an inlet air temperature of 145 °C, a rotating atomizer of 10 × 10 kPa, a pump speed of 1.5 mL/min, and a blower speed of 0.6 m³/min was used for this purpose.

In two FD and SD encapsulation methods, the optimal microcapsules with the highest encapsulation efficiency (EE%) and Chl content (CC μg/mL) were investigated for further analysis. EE was measured according to the following Eq (1):

$$\text{Encapsulation efficiency} (\%) = \frac{\text{Total chlorophyll amount} - \text{Surface chlorophyll amount}}{\text{Total chlorophyll amount}} \times 100 \qquad (1)$$

The sum of the surface chlorophyll (SC), core chlorophyll (CC), and residual chlorophyll (RC) in the supernatant of fresh microcapsules gives the Total chlorophyll (TC). The amount of CC in the microcapsules was obtained by centrifuging the fresh microparticle suspension at 10,000 rpm for 15 min to get the pellet. UV–vis spectrophotometer was used to immediately determine Chl in the supernatant. SC assessment was done via pipetting 10 mL of hexane into the microparticles and then gently shaking for five min. Then, following its centrifuge, the supernatant was measured to determine the SC content. After pipetting 20 mL of acetone 80 % into the pellets, they were ultrasonicated (100 % power) for 30 min at room temperature aimed at breaking the Chl-M membrane and discharging CC. Finally, the suspension was centrifuged and the supernatant's CC was determined. To ensure the complete extraction of Chl from Chl-M, the process was repeated three times to achieve colourless microcapsules. The optimal formulation table to produce microcapsules by two encapsulation methods is shown in Table 1.

Table 1
Optimal microcapsules produced by spray-drying and freeze-drying methods and values of the response at optimal conditions.

	MD (g)	WPI (g)	Chl (g)	EE (%)	CC (μg/mL)
FDM	17.27	11.21	22.05	90.46 ± 0.62	85.85 ± 0.43
SDM	16.02	16.57	20.40	90.27 ± 0.21	55.36 ± 0.36

2.4. Characterization of Chl-Ms

2.4.1. Particle size analysis of Chl-Ms

A dynamic light scattering type zetasizer (Microtrace MRB, S3500, USA) was used to analyse the particle size distribution. In this test, polydispersity index (PDI), mean particle size, and ζ-potential were evaluated before and after drying. For this purpose, microcapsules and emulsion before drying were used. A small amount of microcapsules was dispersed in distilled water to avoid multiple scattering effects. All tests were performed at 25 °C and the average of three readings was reported.

2.4.2. Apparent colour analysis of Chl-Ms

The Hunter Lab colourimeter (Hunter Lab, colourFlex, USA) was used to determine the colour of Chl extract with solvent, pure Chl extract and Chl-Ms. First, after dissolving 0.5 g microcapsules in 50 mL distilled water and transferring it to a cuvette for measurement, L*, a* and b* parameters in the form of reflectance specula were obtained utilizing the light source D65 and observation angle of 10°. The lightness of the colour lightness is represented by the L* (0 black − 100 white), the colour between green (−) and red (+) is represented by and the colour between blue (−) and yellow (+) is represented by b*. Finally, Eq (2) (Zhang et al., 2022) was used to calculate the total colour difference (△E*):

$$\Delta E = \sqrt{\Delta a^{*2} + \Delta b^{*2} + \Delta L^{*2}} \quad (2)$$

where △E* denotes the total colour difference, △L* is the difference between control L* and sample L*, △a* represents the difference between control a* and sample a*, and △b* shows the difference between control b* and sample b*.

2.4.3. Fourier transform infrared spectroscopy (FT-IR)

FT-IR spectra of Chl-Ms, Chl, and carrier agents (WPI and MD) were investigated by employing the FT-IR spectrometer (Shimadzu 8400 model, Japan) in the region of 4000—400 cm^{-1}. The analysis was done at ambient temperature.

2.4.4. Differential scanning calorimetry (DSC)

DSC analyses were performed for Chl and Chl-Ms utilizing a DSC (Mettler Toledo, Swiss) instrument calibrated with indium. First, after placing 20 mg of each sample onto a standard aluminium pan, they were heated from 25 to 350 °C at a heating rate of 10 °C/min under constant nitrogen purging at a flow rate of 50 mL/min. An empty sealed aluminium pan was utilized as a reference (Kang et al., 2019).

2.4.5. Scanning electron microscopy (SEM)

The morphology of Chl-Ms was observed by a SEM (Philips XL30 ESEM, Netherlands). A sputter coater was used to coat Chl-Ms with a thin conductive layer of gold for 15 s. Then, the coated Chl-Ms was observed at an accelerating voltage of 10 kV.

2.4.6. X-ray diffraction (XRD) pattern

An X-ray diffractometer (Xpert Pro MPD, Netherlands) was used to investigate the crystal structure of Chl-Ms investigated with. Cu-Kα at 40 kV and 15 mA was utilized as the radiation source, and the collection of XRD pattern was carried out in the 2θ range from 2 to 80° at a scan rate of 0.2°/min with a step width of 0.02° (Zhang et al., 2020).

2.4.7. Stability test (light, pH) of Chl-Ms

The light effect on the unencapsulated Chl and Chl-M was studied. First, after dispersing 50 mg of Chl-M and unencapsulated Chl (control) in 10 mL of 5 % ethanol, the samples were maintained at room temperature with bright sunshine for 21 days. Finally, Eq (3) was used to measure the percentage of Chl retained:

$$\text{Chlorophyll retention}(\%) = \frac{\text{residual chlorophyll content}}{\text{initial chlorophyll content}} \times 100 \quad (3)$$

The method developed by (Agarry, Wang, Cai, Wu, et al., 2022) with modification was hired to investigate the effect of pH on unencapsulated Chl and Chl-M. The studied pH levels were 2, 4, and 6, all examined in triplicate. In the current work, edible citric acid buffers (Merck, Germany) were implemented. After preparing 40 mL of each edible citric acid buffer of pH 2, 4, 6 and 8, 50 mg of unencapsulated Chl (control) and Chl-Ms were homogenized in them at 3000 rpm for 5 min utilizing a vortex apparatus. The Chl-Ms were centrifuged, and the residual Chl content was evaluated.

2.4.8. Stability test at different temperatures

After weighing 50 mg of Chl-M into capped vials, they were stored in the dark, in the incubator at 25, 50, 75 and 100 °C for 10 days. The withdrawal of the samples was done at two-day intervals, aimed at monitoring the degradation of Chl-M. Following the dispersion of the withdrawn samples into 20 mL of 80 % acetone by vertexing at 3000 rpm for 2 min, they were transferred to an ultrasonic bath (Elma S30H model) at 100 % power for 30 min. Then, the suspension was centrifuged at 10,000 rpm for 15 min. The replication of the procedure was carried out until the colourless microparticles appeared. Eq (4) was utilized to analyse the Chl extract for Chl content at absorbances of 665 and 649 nm:

$$\text{Chlorophyll}(\mu g/mL) = 6.10 \times A_{665} + 20.04 \times A_{649} \quad (4)$$

The first-order kinetic model of Eq (5) was used to evaluate Chl degradation:

$$\ln C = \ln C_0 - K(t) \quad (5)$$

where C_0 and C are the initial Chl concentration and Chl concentration at time t, respectively, t represents the storage time and k (hr^{-1}) denotes the degradation rate constant. The slope of the plots of $\ln C/C_0$ vs. t at the different studied temperatures of 25, 50, 75, and 100 °C were used to calculate the Chl degradation rate constants.

The Eq (6) and Eq (7) were used to calculate the half-life ($t_{1/2}$) and decimal reduction time (D) of Chl-Ms:

$$D = \frac{\ln 10}{k} \quad (6)$$

$$t_{1/2} = \frac{\ln 2}{k} \quad (7)$$

2.5. Statistical analysis

All experiments were replicated at least three times for each treatment and all results were reported as the mean ± standard deviation. A one-way ANOVA of the SPSS 27.0 software version was used to evaluate significant differences (p < 0.05) among samples. Differences between means were identified using Duncan's multiple comparison test.

3. Results and discussion

3.1. Particle properties

The measurement of microcapsule particles is extremely important because these particles affect the texture of food that is added to it. Microcapsules dried by the FD method are usually used in the food and pharmaceutical industries. The advantage of this method is it makes the microcapsules more stable by reducing their agglomeration (Mehnert & Mäder, 2012). ζ-potential is a factor for the potential stability of the colloidal system. It is a measure of net surface charge and a key factor in predicting the stability of microparticles. Generally, the limit of stability and instability of suspension can be determined in terms of ζ-potential. The higher the ζ-potential, the lower the chances of particle aggregation occurring due to electric repulsion (Seyfoddin & Al-Kassas, 2013).
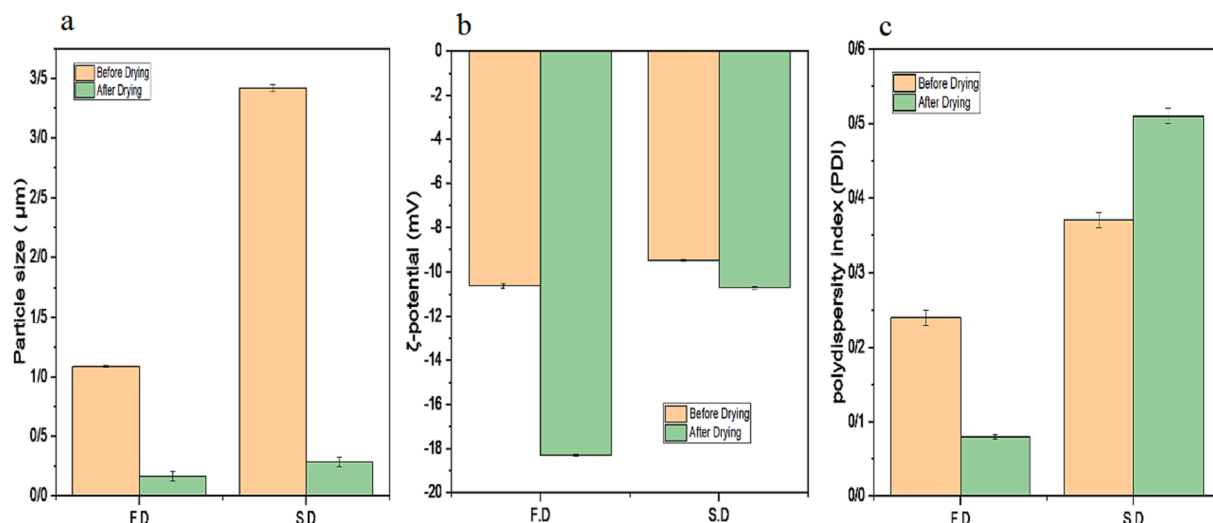
Fig. 1. The effect of encapsulation process on (a): particle size, (b) ζ-potential, (c) polydispersity index (PDI) before and after drying.

The polydispersity index (PDI) is very important in the evaluation of the homogeneity and stability of the particle size distribution. Samples with a wider variety of sizes have a higher PDI value than samples with uniform-sized particles, hence the PDI value measures the particle size distribution (Ahmadian et al., 2024).

In the current work, the particle size in FD changed from 1.087 to 0.165 μm and in SD from 3.420 to 0.285 μm (Fig. 1a). PDI of microcapsules after FD changed from 0.24 before drying to 0.08 after drying and in SD samples from 0.37 before drying to 0.51 after drying (Fig. 1c).

Different particle size distribution, particularly influenced by the two techniques, was attributed to the wall material ratio and processes utilized. The difference in particles' size before the drying process was justified by the difference in the ratio of the primary emulsion compounds based on Table 1. MD with a high degree of hydrolysis also produces smaller particles (Tonon et al., 2010). The microcapsules' particle size in the SD was determined according to the initial emulsion and atomization (Walton, 2000).

FD did not change the morphological properties and the crystallinity of the samples, but the particle size greatly decreased in comparison to other drying methods (Piazza et al., 2020). In their study, Wang et al stated that the advantage of FD is to improve the stability of microparticles by reducing aggregation. One possible reason for the reduction in particle size during encapsulation by FD compared to SD is the use of the freeze–thaw process. In FD, samples are individually frozen and then dried under low pressure and temperature. This process can cause cell rupture and improve the dried environment inside the capsule, which can result in a decrease in particle size. In contrast, in SD, samples are sprayed as a liquid and then dried under high heat. This process may lead to particle aggregation, which can result in larger particle sizes being maintained (Walton, 2000). Therefore, it can be said that in FD, the polydispersity index will be more uniform. Therefore, the mechanism of action for the change in PDI during encapsulation by FD and SD is related to the differences in particle formation and drying conditions between the two methods. ζ-potential for FD varied from −10.6 to −18.3 mV and for SD from −9.5 to −10.7 mV (Fig. 1b). The rise in ζ-potential in the modulus after FD and SD could be a reflection of reconfiguration in the surface coverage and the broader unfolding of anionic groups during the drying process (Agarry, Wang, Cai, Kan, et al., 2022).

3.2. Appearance colour of Chl-Ms

The type of treatment conditions, type and concentration of carrier and core materials, natural colour (wall or core material), and

Table 2
The effects of different treatments on the colour properties (L*, a*, b* and △E*) of Chl-Ms.

Drying process	Sample	L*	a*	b*	△E*
Freeze drying	Extract with solvent	40.499 ± 0.271[h]	−19.509 ± 0.382[a]	38.503 ± 0.253[g]	32.321 ± 0.280[f]
	Pure extract (control)	17.416 ± 0.267[a]	−0.023 ± 0.006[g]	27.007 ± 0.295[a]	NA
	Extract after freeze-drying	30.759 ± 0.144[e]	−6.244 ± 0.250[d]	35.037 ± 0.474[e]	16.769 ± 0.257[c]
	Freeze emulsion	21.231 ± 0.250[b]	−12.434 ± 0.250[c]	28.72 ± 0.402[b]	13.096 ± 0.063[b]
	FDM*	24.361 ± 0.283[d]	−3.087 ± 0.238[f]	32.427 ± 0.480[d]	9.327 ± 0.267[a]
Spray drying	Extract after spray drying	34.194 ± 0.252[f]	−5.641 ± 0.327[e]	36.555 ± 0.377[f]	20.105 ± 0.125[d]
	Spray emulsion	23.496 ± 0.287[c]	−15.314 ± 0.392[b]	31.107 ± 0.263[c]	16.958 ± 0.284[c]
	SDM**	35.363 ± 0.258[g]	−6.843 ± 0.406[d]	36.092 ± 0.226[f]	21.233 ± 0.270[e]

Different letters in the same column indicate significant differences (p < 0.05).
*: freeze dried microcapsules, **: spray dried microcapsules.
NA: not available.

denaturation/thermal decomposition during drying all should be considered in determining the appearance colour of microcapsules (Zhang et al., 2020). In this study, the colour of Chl solution was evaluated in several stages: after extraction with solvent, pure Chl extract after desolvation, emulsion before drying, and microcapsule colour after drying Table 2. The colour of Chl without capsule was dark green, whereas that of Chl-Ms was lighter than the sample without capsule. Different colours of Chl-Ms might be attributed to the dilution effect of the wall materials and the encapsulation impact of the mutual reaction between the wall materials and Chl.

Compared to the colour of the control sample (pure Chl extract after desolvation), the L* value of the emulsion and Chl-Ms increased and a* significantly decreased (p < 0.05), which confirms that the product's light green colour was derived from Chl. The higher the Chl concentration, the sample had a lower L*. In the current work, the difference in main colour was owing to obtaining microcapsules with different drying methods. All samples presented high L* values compared to the control sample. For FDM, L* values were lower than SDM and its b* values were higher than the control sample and lower than the SD sample and it had a darker appearance than SDM; this difference could be attributed to the drying process. The type of drying process and the percentage of wall

material affected the colour intensity of the samples.

The Chl extract before desolventization had a brighter appearance with a higher L*, but when the extract was desolvated and the intensity of Chl increased, L* decreased and the sample became darker because the extracted Chl had a dark green colour. Next, when it was combined with the walls for encapsulation, the intensity of the dark colour was reduced and the colour of the sample became lighter, confirmed by the increase of L*. This matter has also been stated in the research of (Zhang et al., 2020), (Kang et al., 2019) and (Ahmed et al., 2010), reporting that the addition of a wall caused an increase in L* in microcapsules. The difference in the L*, a* and b* factors of the two freeze and spray emulsion samples before drying could also be due to the difference in the percentage of wall and core compositions according to Table 1. Since WPI had a yellower appearance than MD, its increase in the emulsion caused an increase in b* in the SD. The concentration of the core was also effective in the colour of the emulsion before drying. The negativity of a* in microcapsules indicated that the samples were green due to the integration of Chl in different wall materials.

In SD, the use of high temperature for drying caused a significant loss of Chl due to the thermal destruction of Chl pigments, making the colour of the SDM lighter compared to the FDM. In △E* of the samples, we also saw that the higher the concentration of the sample (in terms of Chl content), the lower the △E* i.e., the difference with the control sample (the same extracted Chl extract) was smaller.

3.3. FT-IR of Chl- Ms

The reactions or interactions occurring during the encapsulation can affect the structure of wall materials, the encapsulated material, and the microcapsule (Comunian & Favaro-Trindade, 2016). FT-IR spectroscopic analysis was carried out to characterize the intermolecular interactions between the core and wall materials (Fig. 2a). This method is a proficient tool to identify unknown compounds in a substance. In the MD spectrum, absorption bands were seen at 1356 (O—H bending), 1636 (C=O stretching), 2924 (C—H stretching), 3282 (O—H stretching), and 1410 (CH$_2$ bending). The peak at 1147 indicated C—O stretching and C—O—H bending, while the peaks at 928, 847, 761, 759, and 701 are ascribed to pyranoid ring skeletal vibrations. In the WPI spectrum in the wavenumber (cm^{-1}) range of 3000–3600, two peaks with wavenumbers of 3052 and 3270 corresponding to –OH and –NH stretching were observed. Amide bands I and II are the most important vibrational bands of the protein skeleton. The amide I band (range 1600–1700 cm^{-1}) was related to stretching vibrations of C=C peptide bond and was sensitive to the second structure of the protein, while the Amide II band (1500–1400 cm^{-1}) was due to in-plane bending –NH (40–60 %) and stretching vibration –CN (18–40 %).

Chl bands at 3455 (O—H stretching), 2921 (C—H stretching in phytol), 2852 (asymmetric and symmetric CH$_2$ and CH$_3$ stretching), 1730 (C-173 = O and C-133 = O stretching), 1690 (C-131 stretching = O), 1610 (C=C and C≡N skeletal stretching in the Chl ring system), and 1280 (C-173-O and C-133-O stretching) appeared, in a good agreement with the results of a previous study (Kang et al., 2019; Zhang et al., 2022; Zhang et al., 2020).

Comparing the peaks observed in the Chl sample with the FDM and SDM showed that the intensity of the band decreased at 2852 and 2921, respectively. The decrease in the vibration of methylene and methyl groups could be attributable to the interaction of Chl phytol group as core and hydrophobic region of MD and WPI as wall. The characteristic hydroxyl peaks (O—H stretch) were seen around 3400 cm^{-1} for all microcapsules. In contrast with the peak intensity for WPI and MD, the intensity of hydroxyl peaks witnessed a significant fall for all microcapsules, meaning that the hydroxyl groups in WPI and MD engaged in chemical reactions during SD and FD, such as esterification between MD and WPI and/or hydrogen bonding. In the Chl sample, band 1730 was observed more intensely, but the intensity of this band was very insignificant in the produced microcapsules, likely owing to the combination
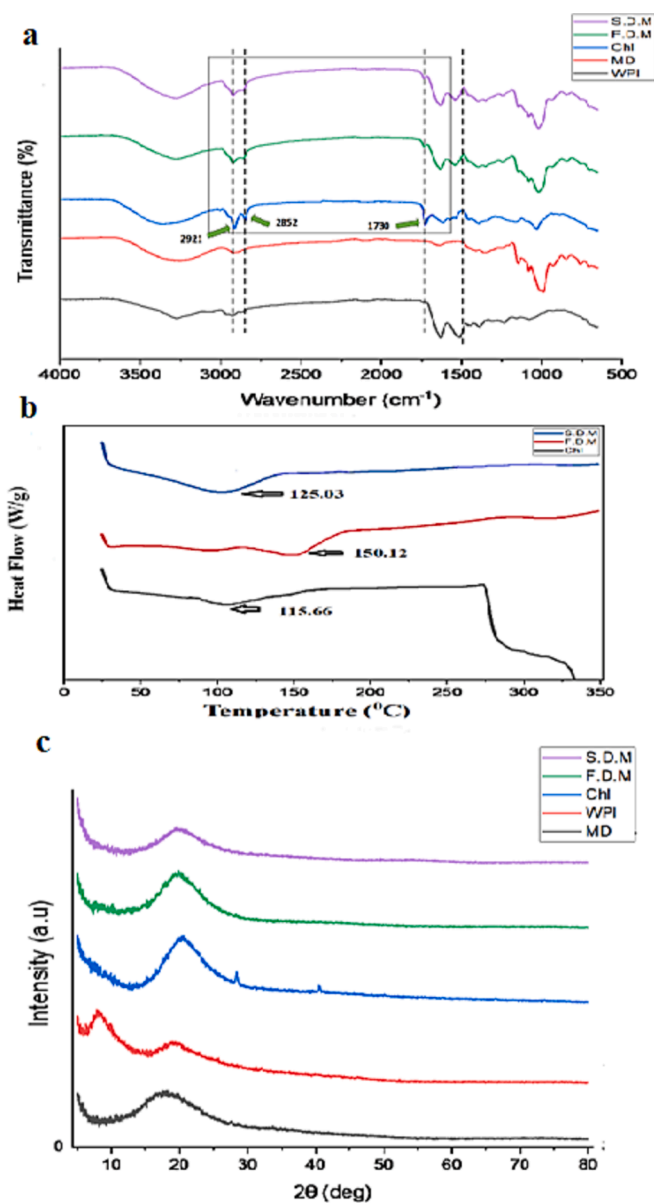

Fig. 2. FT-IR (a), DSC (b) and XRD (c) spectra of chlorophyll (Chl), whey protein isolate (WPI), maltodextrin (MD), and microcapsules prepared using FD (freeze drying) and SD (spray drying) methods.

of the ester bond of the pyrrole ring and the walls of MD and WPI. By observing the change in the intensity of the bands or the creation of new bands in the Chl-Ms compared to the sample of Chl, WPI and MD, it could be concluded that the interaction between the core and the wall had been formed. Based on the spectrum of Chl, the mentioned peaks indicated the presence of Chl in all microcapsules. As a result, the successful microcapsulation with FD and SD was confirmed.

3.4. Differential scanning calorimetry (DSC)

DSC is an essential proficient technique to evaluate the physical state of the wall material and core, associate the behaviour of heat flow and different temperatures, and obtain information such as melting and crystallization temperature as well as glass transition temperature (Comunian & Favaro-Trindade, 2016). The thermal behaviour of Chl and Chl -Ms coated with WPI and MD prepared by FD and SD methods evaluated by DSC is depicted in Fig. 2b. In the Chl sample, an endothermic peak was observed at 115.66 °C. According to several studies

(Agarry, Wang, Cai, Wu, et al., 2022; Guad et al., 2006; Kang et al., 2019), this peak could be related to the melting of Chl (The melting point range of Chl was reported to be 117–133 °C). FDM and SDM showed endothermic peaks at 150.12 °C and 125.03 °C, respectively, probably related to the melting point of Chl-M.

Wall materials restrict the mobility of the Chl molecules, preventing them from interacting with each other and forming aggregates that can lower the melting temperature. Furthermore, the wall materials used for encapsulation can also have a higher melting temperature than Chl, contributing to the overall increase in melting temperature of the Chl-M. This is because MD and WPI are both high molecular weight compounds that can withstand high temperatures without degrading or melting.

The FDM and SDM showed different melting peaks. The composition percentage of the wall material could affect this matter. The FDM method had a higher percentage of MD than the SDM (according to Table 1). The melting point of MD has been mentioned in previous studies 209 °C (Kang et al., 2019). Therefore, increasing the amount of MD in FDM increased the melting point of this microcapsule compared to SDM. No endothermic peak of Chl was observed in the DSC thermograms of all microcapsules, confirming good coverage of the core material with the wall material and the presence of Chl in the non-crystalline state (Zhang et al., 2021).

3.5. Morphology of Chl-Ms

Fig. 3 depicts the SEM micrographs of microcapsules achieved utilizing different mixtures of wall materials (WPI & MD) consisting of Chl via two methods, FD and SD. Besides their difference in particle size, consistent with the particle size distribution patterns of Fig. 1, microparticles produced by the two drying techniques presented different morphological characteristics. SDM had a more regular and spherical shape, with a relatively smoother surface compared with the FDM, exhibiting more cracks or fractures. The formation of dimples in the samples' surface dried by SD is dependent on the drying parameters, the composition of the wall material and the diameter of the emulsion particles (Hashemiravan et al., 2013).

The wrinkles and dimples that appeared on the surface of SDM can be likely due to the rapid evaporation of water during SD, which mainly occurs owing to the rapid formation of a crust on the droplets' surface in the initial stages of drying. Scanning electron micrographs showed SDM had a spherical structure, and those obtained from FD, were of irregular and glassy structure. According to the morphology of the microcapsules, the Chl-Ms produced by the FD had more pores than the that produced by the SD method. In the FD method, the reason behind the porous form was ice crystal formation during freezing and the sublimation process during drying (Kurniasih et al., 2018). A brittle matrix was formed after drying.

3.6. XRD pattern of Chl-Ms

The encapsulation impacts on the Chl crystallinity are reflected by the XRD pattern in Fig. 2c. As the microcapsules' crystallinity is associated with their stability, it is imperative to find out if the microcapsules have crystalline or amorphous structures via XRD analysis. In General, the diffuse and broad peaks in the XRD profile reflect amorphous structures since amorphous materials are disordered yielding dispersed bands. Nonetheless, crystalline materials present sharp and defined peaks attributed to their well-ordered state. Fig. 2c shows the XRD profiles of Chl-Ms, MD, WPI and Chl, and loaded with WPI&MD through FD and SD methods. The Chl sample presented 3 peaks at $2\theta = 22°$, $29°$ and $41°$, which showed an amorphous structure with minimal crystallinity. The WPI showed two peaks at $2\theta = 9°$ and $20°$. FDM and SDM and MD showed an amorphous structure with minimal organization, as shown by the presence of broad peaks. Several studies (Botrel et al., 2014; Kang et al., 2019; Silva et al., 2013) have also mentioned the amorphous structures of MD and the lack of effect of the drying process,
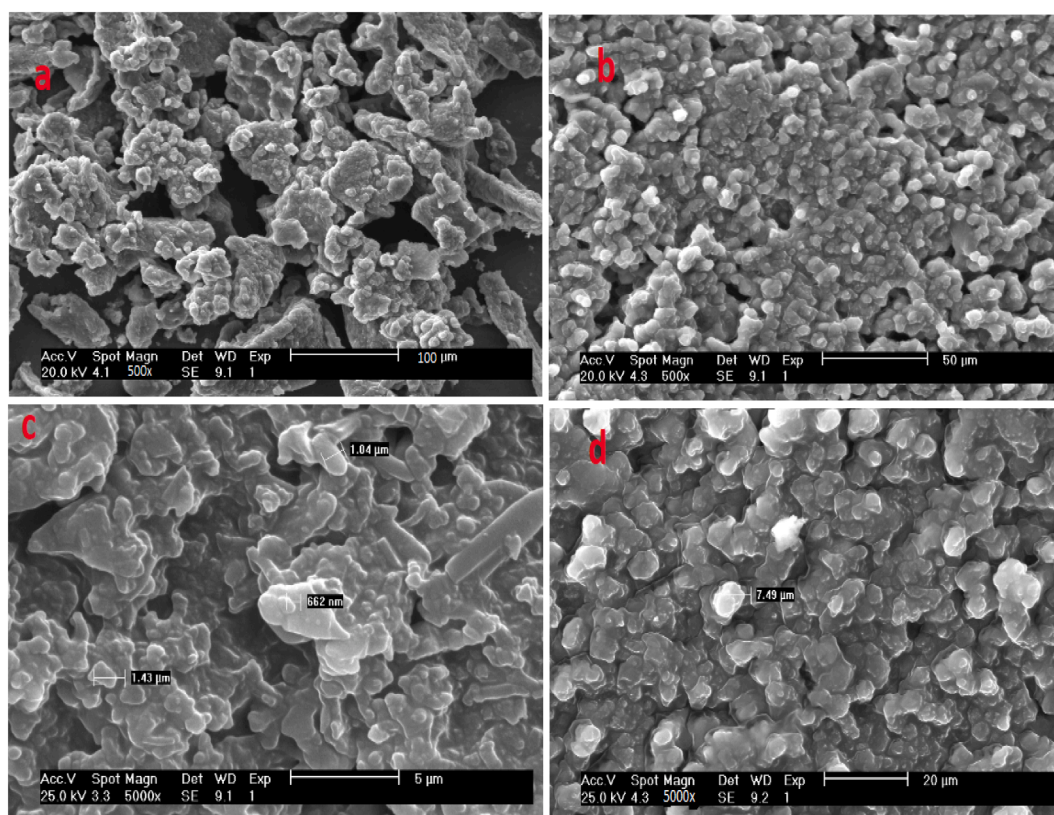

Fig. 3. SEM images of chlorophyll microcapsules (Chl-Ms) produced by: (a, c) FD (freeze drying) and (b, d) SD (spray drying) with magnification 500× and 5000×.

on the crystalline characteristics of the wall material. In their research, (Zhang et al., 2020) and (Zhang et al., 2017) mentioned 2 specific diffraction peaks for WPI at 8.9° and 19.6°; in a good agreement with the results of this research. In the XRD profiles of SDM and FDM, the specific peaks of Chl disappeared. The finding data, particularly those obtained by DSC analysis, further confirmed the large embedment of Chl in the wall materials composed of MD and WPI (Fig. 2b). It means that the formation of chlorophyll-loaded microcapsules was further proven. In general, an increase in the sharpness of the diffraction peaks in XRD profiles confirms a higher degree of crystallinity of the sample (Wei & Periasamy, 2011). Based on this, it was shown that the FDM showed more crystallinity compared to the SDM given the higher content of MD in the wall material. In addition, the amorphous and crystalline conditions depend on the storage stability and physicochemical properties of powders. Compared to amorphous, crystal state has less dissolution and hygroscopy. Water absorption of materials is associated with weight gain, microstructural collapse, nutrient degradation, and potential microbiological instability during storage (Borrmann & Rocha, 2012; Nambiar et al., 2017). Therefore, the XRD results showed that the FDM might have higher storage stability due to its increased degree of crystallinity in contrast with SDM.

3.7. Stability test (light and pH) of Chl-Ms

Light can break the chemical structure of pigments and change their chemical structure, making them colourless in a process called photodegradation. The electromagnetic spectrum of the sun contains long wavelengths from gamma to radio waves. The energy of UV waves of the sun plays the main role in accelerating colour fading. The photon energy of these waves, not absorbed by ozone in the earth's atmosphere, is more than the energy of dissociation of single carbon–carbon bonds in the structure of pigments, causing these bonds to break; as a result, the colour fades. Accordingly, the effect of the sun's ultraviolet rays on pigments containing carbon is greater, so organic pigments are less resistant to light than mineral pigments (Groeneveld et al., 2022). When exposed to a vital factor like light, Chl, as a natural pigment and bioactive compound, undergoes a variety of chemical reactions such as oligomerization, isomerization and oxidation.

Chl is a main photosynthetic pigment; it can transfer light energy to a chemical receptor via alterations in its molecular structure. Thus, its structural stability can be evaluated by the amount of Chl remaining after exposure to light (Agarry, Wang, Cai, Kan, et al., 2022). following 3-week exposure of unencapsulated Chl to sunlight at room temperature, only 1.84 % of free Chl was retained, while FDM and SDM showed significant ($p < 0.05$) protection for Chl with 38.12 % and 29.38 % at the end of the same period (Fig. 4a), showing that the produced Chl-Ms were enough to keep Chl away from bad light conditions. Photooxidation is called oxidation due to activated oxygen by coloured compounds such as Chl, In other words, a combined reaction with oxygen in the presence of light. Chl can be protected from bad light conditions and have a longer shelf-life during storage via microencapsulation and possible hydrogen bonding with MD and WPI complexes. FD had higher Chl retention ($p < 0.05$) than SD. Smaller particle size and higher ζ-potential of FDM (according to section 3.1), considered indicators for the stability of superior particles, could be attributed to the higher stability of these microcapsules. Also, MD with high DE content has free reducing groups that can act as an antioxidant (Bae & Lee, 2008).

It is vital to study stability as a function since changes in pH in the processing environment can cause alterations in microcapsules and lead to degradation or release of core materials from encapsulating agents. Chl is unstable under the influence of acidic conditions; its magnesium atom is replaced by two hydrogen ions, and pheophytin, whose colour is olive-brown, is produced. Therefore, in the present study, we investigated the pH impact on the stability of Chl and Chl-Ms. Considering the pH environment of the main human digestive organs (stomach: pH 1.5–4.0; oral cavity: pH 6.5–7.5; intestine: pH 4.0–7.0), pH values of
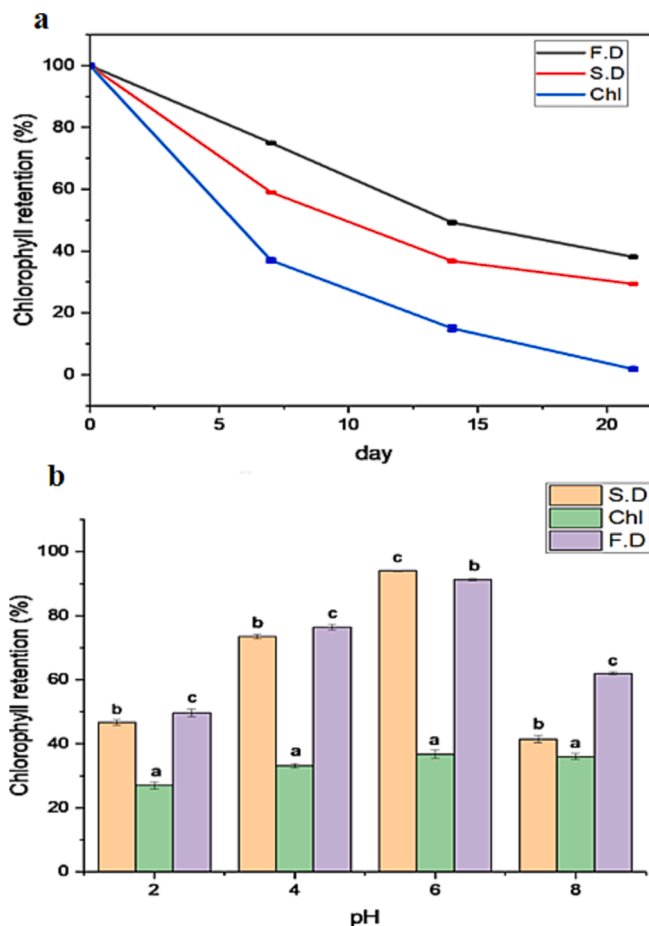
Fig. 4. The chlorophyll retention (%) of chlorophyll (Chl) and chlorophyll microcapsules (Chl-Ms) produced by two methods FD (freeze drying) and SD (spray drying) under different storage conditions (a): light, (b): pH.

2,4,6,8 were tested. Fig. 4b depicts the stability of FDM and SDM against pH changes, expressed as retention percentage. The retention rate of free Chl under acid stress was 27.3 % to 36.03 % respectively, significantly lower than any of the Chl-Ms. These results confirmed that the chemical stability and retention rate of Chl experienced a significant increase ($p < 0.05$) after encapsulation utilizing WPI and MD as wall materials. The retention of Chl particles produced by FD and SD varied from 49.67 % to 91.28 % and 41.47 %-94.04 %, respectively. The increased stability of Chl-M against pH fluctuations can be attributed to the isoelectric pH of MD (5.2–6.8) and WPI (6.5) (Khaire & Gogate, 2019), which create an almost neutral environment around Chl and thus increase stability. The FDM presented significantly higher retention at all pH levels except pH 6 ($p < 0.05$). The higher stability of the FDM against acidic pH makes it a proper option to use a wider range of food products, including high-acid foods.

3.8. Evaluation of storage stability at different temperatures

The temperature of storage plays a key role in preserving heat-sensitive substances like flavours and nutrients. Highly-stable microcapsules can have significantly increased use in industrial processing (Zhang et al., 2022). Thus, the effect of storage temperature on the stability of both encapsulated and non-encapsulated Chl was investigated. Dried Chl without capsules and Chl-M were kept at different temperatures (25, 50, 75 and 100 °C) for 10 days in the dark. The first-order kinetic model was used to study Chl degradation. For all temperature conditions studied in this research, Chl degradation in loaded Chl microparticles fitted well in the first-order kinetic model with

Table 3

Thermal degradation kinetics of Chl and Chl-Ms produced by FD and SD during storage at 25, 50, 75 and 100 °C using MD and WPI as wall materials.

Temperature	System	k (hr^{-1})	Correlation coefficient(r^2)	D (hr)	$t_{1/2}$ (hr)
25	Chl[1]	0.00304 ± 0.0057[c]	0.93	756.57 ± 0.156[a]	227.96 ± 0.298[a]
	FDM[2]	0.00141 ± 0.0057[a]	0.99	1631.20 ± 0.010[c]	491.48 ± 0.052[c]
	SDM[3]	0.00180 ± 0.0088[b]	0.95	1277.77 ± 0.107[b]	385 ± 0.360[b]
50	Chl	0.00456 ± 0.0011[c]	0.97	504.38 ± 0.110[a]	151.97 ± 0.085[a]
	FDM	0.00202 ± 0.00013[b]	0.96	1138.61 ± 0.105[b]	343.06 ± 0.102[b]
	SDM	0.00176 ± 0.00021[a]	0.91	1306.81 ± 0.100[c]	393.75 ± 0.132[c]
75	Chl	0.00533 ± 0.0053[c]	0.98	431.51 ± 0.328[a]	130.01 ± 0.586[a]
	FDM	0.00211 ± 0.0021[b]	0.96	1090.04 ± 0.450[b]	328.43 ± 0.254[b]
	SDM	0.00201 ± 0.0020[a]	0.96	1144.27 ± 0.300[c]	344.77 ± 0.334[c]
100	Chl	0.00611 ± 0.0002[c]	0.91	376.43 ± 0.352[a]	113.42 ± 0.236[a]
	FDM	0.00418 ± 0.0001[b]	0.90	550.23 ± 0.701[b]	165.78 ± 0.541[b]
	SDM	0.00353 ± 0.0002[a]	0.87	651.55 ± 0.250[c]	196.31 ± 0.193[c]

1: chlorophyll.
2: freeze dried microcapsule.
3: spray dried microcapsule.

correlation coefficient (r^2) values between 0.87 and 0.99 (Fig. S1). Table 3 presents the thermodynamic parameters of loaded Chl-M. The rate constant (k) can be utilized to predict Chl degradation as a function of heat i.e., a decrease in k value results in higher stability of the Chl. A rise in temperature increased k values for all different Chl-Ms. Higher temperatures raised the degradation rate due to an increase in the frequency of molecular collisions (Kuck et al., 2017). Chl-Ms showed a lower K value and, as a result, higher thermal stability than the Chl sample without capsules. The SDM shows a significantly (p < 0.05) lower k value at 50, 75 and 100 °C, more stable compared to FDM and Chl to Chl degradation at higher temperatures.

D-value shows the time needed to degrade 90 % of the Chl compound in the microcapsule at a certain temperature. The D-value, ranging from 376.43 to 1631.20 hr for all investigated temperatures, witnessed a decrease with an increase in temperature. The FDM showed higher stability against Chl degradation at 25 °C, but with an increase in temperature, we saw an increase in the stability of the SDM due to having less K. According to the D-values, a similar trend was observed for $t_{1/2}$. Half-life ($t_{1/2}$) corresponds to the time at which the initial content is reduced by 50 % concerning zero time. $t_{1/2}$ values ranging from 113.42 to 491.48 hr for all temperature conditions, with free Chl at 100 °C having the lowest half-life among samples. FDM had the highest half-life at 25 °C.

Products dried by SD have important and very desirable properties such as better solubility, lower humidity and higher thermal stability (Stefanescu, 2010) and this issue can be a reason for increasing the stability of SDM compared to FDM at higher temperatures. Both produced microcapsules showed significant thermal stability (p < 0.05) compared to free Chl. The interaction between wall materials was beneficial to improve the thermal stability of Chl-M. MD and WPI are hydrophilic materials that can form a protective layer around the Chl molecules during the encapsulation process. This layer can prevent the Chl from being exposed to external factors such as heat, which can cause degradation and reduce its stability.

4. Conclusions

The use of MD and WPI as a carrier and FD as an encapsulation method increased the stability of Chl against stresses such as pH change and light. By examining the results of the XRD test, it could be concluded that the FDM could have a higher storage stability due to their higher crystallinity. During the production of Chl-Ms by the FD method, due to the lack of high temperature (a critical factor for Chl), the Chl content was higher, and as a result, the colour of FDM was also darker. The FDM had the highest melting point compared to Chl and SDM. Putting the results of the tests together, it can be said that Chl encapsulated with MD and WPI walls by FD method can be used as a colour additive with high efficiency in the food industry. Of course, there is a need to investigate the release pattern of Chl in the digestive tract in simulated digestive conditions during future studies.

CRediT authorship contribution statement

Shahrbanoo Amadi Ledri: Conceptualization, Formal analysis, Writing – original draft. **Jafar M. Milani:** Conceptualization, Resources, Supervision, Writing – review & editing. **Seyed-Ahmad Shahidi:** Conceptualization, Resources. **Abdolkhaleg Golkar:** Conceptualization, Resources.

Declaration of competing interest

The authors declare that they have no known competing financial interests or personal relationships that could have appeared to influence the work reported in this paper.

Data availability

Data will be made available on request.

Acknowledgement

Appendix A. Supplementary data

Supplementary data to this article can be found online at https://doi.org/10.1016/j.fochx.2024.101156.

References

Abbasi, A., Emam-Djomeh, Z., Mousavi, M. A. E., & Davoodi, D. (2014). Stability of vitamin D3 encapsulated in nanoparticles of whey protein isolate. *Food Chemistry, 143*, 379–383. https://doi.org/10.1016/j.foodchem.2013.08.018

Agarry, I. E., Ding, D., Cai, T., Wu, Z., Huang, P., Kan, J., & Chen, K. (2023). Inulin–whey protein as efficient vehicle carrier system for chlorophyll: Optimization, characterization, and functional food application. *Journal of Food Science, 88*(8), 3445–3459.

Agarry, I. E., Wang, Z., Cai, T., Kan, J., & Chen, K. (2022). Chlorophyll encapsulation by complex coacervation and vibration nozzle technology: Characterization and stability study. *Innovative Food Science & Emerging Technologies, 78*, Article 103017. https://doi.org/10.1016/j.ifset.2022.103017

Agarry, I. E., Wang, Z., Cai, T., Wu, Z., Kan, J., & Chen, K. (2022). Utilization of different carrier agents for chlorophyll encapsulation: Characterization and kinetic stability study. *Food Research International, 160*, Article 111650. https://doi.org/10.1016/j.foodres.2022.111650

Ahmadian, S., Kenari, R. E., Amiri, Z. R., Sohbatzadeh, F., & Khodaparast, M. H. H. (2024). Fabrication of double nano-emulsions loaded with hyssop (Hyssopus officinalis L.) extract stabilized with soy protein isolate alone and combined with chia seed gum in controlling the oxidative stability of canola oil. *Food Chemistry, 430*, Article 137093.

Ahmed, M., Akter, M. S., Lee, J.-C., & Eun, J.-B. (2010). Encapsulation by spray drying of bioactive components, physicochemical and morphological properties from purple sweet potato. *LWT-Food Science and Technology, 43*(9), 1307–1312. https://doi.org/10.1016/j.lwt.2010.05.014

Apintanapong, M., & Noomhorm, A. (2003). The use of spray drying to microencapsulate 2-acetyl-1-pyrroline, a major flavour component of aromatic rice. *International Journal of Food Science & Technology, 38*(2), 95–102.

Bae, E., & Lee, S. J. (2008). Microencapsulation of avocado oil by spray drying using whey protein and maltodextrin. *Journal of Microencapsulation, 25*(8), 549–560.

Borrmann, D., & Rocha, A. P. T. (2012). Microencapsulation of passion fruit (Passiflora) juice.

Botrel, D. A., de Barros Fernandes, R. V., Borges, S. V., & Yoshida, M. I. (2014). Influence of wall matrix systems on the properties of spray-dried microparticles containing fish oil. *Food Research International, 62*, 344–352. https://doi.org/10.1016/j. foodres.2014.02.003

Chasapis, C. T., Ntoupa, P.-S.-A., Spiliopoulou, C. A., & Stefanidou, M. E. (2020). Recent aspects of the effects of zinc on human health. *Archives of Toxicology, 94*, 1443–1460. https://doi.org/10.1007/s00204-020-02702-9

Chen, L., Remondetto, G. E., & Subirade, M. (2006). Food protein-based materials as nutraceutical delivery systems. *Trends in Food Science & Technology, 17*(5), 272–283. https://doi.org/10.1016/j.tifs.2005.12.011

Comunian, T. A., & Favaro-Trindade, C. S. (2016). Microencapsulation using biopolymers as an alternative to produce food enhanced with phytosterols and omega-3 fatty acids: A review. *Food Hydrocolloids, 61*, 442–457. https://doi.org/10.1016/j.foodhyd.2016.06.003

Domínguez, R., Pateiro, M., Munekata, P. E., McClements, D. J., & Lorenzo, J. M. (2021). Encapsulation of bioactive phytochemicals in plant-based matrices and application as additives in meat and meat products. *Molecules, 26*(13), 3984. https://doi.org/10.3390/molecules26133984

Groeneveld, I., Kanelli, M., Ariese, F., & van Bommel, M. R. (2022). Parameters that affect the photodegradation of dyes and pigments in solution and on substrate–An overview. *Dyes and Pigments, 110999*. https://doi.org/10.1016/j. dyepig.2022.110999

Guad, R., Surana, S., Talele, G., Talele, M. S., & Gokhale, M. S. (2006). *Natural excipients*. Pragati Books Pvt Ltd.

Hanafy, N. A., Leporatti, S., & El-Kemary, M. A. (2021). Extraction of chlorophyll and carotenoids loaded into chitosan as potential targeted therapy and bio imaging agents for breast carcinoma. *International Journal of Biological Macromolecules, 182*, 1150–1160. https://doi.org/10.1016/j.ijbiomac.2021.03.189

Hashemiravan, M., Mazloom, A., & Farhadyar, N. (2013). Nano particles of blueberry in inulin and b-cyclodextrin microencapsules. *International Journal of Nanoscience and Nanotechnology, 9*(4), 185–192.

Hsiao, C.-J., Lin, J.-F., Wen, H.-Y., Lin, Y.-M., Yang, C.-H., Huang, K.-S., & Shaw, J.-F. (2020). Enhancement of the stability of chlorophyll using chlorophyll-encapsulated polycaprolactone microparticles based on droplet microfluidics. *Food Chemistry, 306*, Article 125300.

Hu, Y., Sun, H., & Mu, T. (2022). Effects of different Zn2+ concentrations and high hydrostatic pressures (HHP) on chlorophyll stability. *Foods, 11*(14), 2129. https:// doi.org/10.3390/foods11142129

Kang, Y.-R., Lee, Y.-K., Kim, Y. J., & Chang, Y. H. (2019). Characterization and storage stability of chlorophylls microencapsulated in different combination of gum Arabic and maltodextrin. *Food Chemistry, 272*, 337–346.

Kang, Y.-R., Park, J., Jung, S. K., & Chang, Y. H. (2018). Synthesis, characterization, and functional properties of chlorophylls, pheophytins, and Zn-pheophytins. *Food Chemistry, 245*, 943–950.

Khaire, R. A., & Gogate, P. R. (2019). Whey proteins. In *Proteins: Sustainable source, processing and applications* (pp. 193–223). Elsevier. https://doi.org/10.1016/B978-0-12-816695-6.00007-6.

Kuck, L. S., Wesolowski, J. L., & Noreña, C. P. Z. (2017). Effect of temperature and relative humidity on stability following simulated gastro-intestinal digestion of microcapsules of Bordo grape skin phenolic extract produced with different carrier agents. *Food Chemistry, 230*, 257–264. https://doi.org/10.1016/j. foodchem.2017.03.038

Kurniasih, R., Dewi, E., & Purnamayati, L. (2018). Effect of different coating materials on the characteristics of chlorophyll microcapsules from caulerpa racemosa. IOP Conference Series: Earth and Environmental Science.

Li, F., Zhou, L., Cao, J., Wang, Z., Liao, X., & Zhang, Y. (2022). Aggregation induced by the synergy of sodium chloride and high-pressure improves chlorophyll stability. *Food Chemistry, 366*, Article 130577. https://doi.org/10.1016/j. foodchem.2021.130577

Mehnert, W., & Mäder, K. (2012). Solid lipid nanoparticles: Production, characterization and applications. *Advanced Drug Delivery Reviews, 64*, 83–101.

Mehta, N., Kumar, P., Verma, A. K., Umaraw, P., Kumar, Y., Malav, O. P., Sazili, A. Q., Domínguez, R., & Lorenzo, J. M. (2022). Microencapsulation as a noble technique for the application of bioactive compounds in the food industry: A comprehensive review. *Applied Sciences, 12*(3), 1424. https://doi.org/10.3390/app12031424

Nambiar, R. B., Sellamuthu, P. S., & Perumal, A. B. (2017). Microencapsulation of tender coconut water by spray drying: Effect of Moringa oleifera gum, maltodextrin concentrations, and inlet temperature on powder qualities. *Food and Bioprocess Technology, 10*, 1668–1684.

Ong, C.-L.-Y., Gillen, C. M., Barnett, T. C., Walker, M. J., & McEwan, A. G. (2014). An antimicrobial role for zinc in innate immune defense against group A streptococcus. *The Journal of Infectious Diseases, 209*(10), 1500–1508. https://doi.org/10.1093/infdis/jiu053

Pemmaraju, D., Appidi, T., Minhas, G., Singh, S. P., Khan, N., Pal, M., Srivastava, R., & Rengan, A. K. (2018). Chlorophyll rich biomolecular fraction of A. cadamba loaded into polymeric nanosystem coupled with Photothermal Therapy: A synergistic approach for cancer theranostics. *International Journal of Biological Macromolecules, 110*, 383–391. https://doi.org/10.1016/j.ijbiomac.2017.09.084

Piazza, R. D., Pelizaro, T. A., Rodriguez-Chanfrau, J. E., La Serna, A. A., Veranes-Pantoja, Y., & Guastaldi, A. C. (2020). Calcium phosphates nanoparticles: The effect of freeze-drying on particle size reduction. *Materials Chemistry and Physics, 239*, Article 122004. https://doi.org/10.1016/j.matchemphys.2019.122004

Raei, A., Yasini Ardakani, S. A., & Daneshi, M. (2017). Microencapsulation of the green pigment of alfalfa and its applications on heated food. *Journal of Food Process Engineering, 40*(5), e12529.

Roca, M., Chen, K., & Pérez-Gálvez, A. (2016). Chlorophylls. In *Handbook on natural pigments in food and beverages* (pp. 125–158). Elsevier. https://doi.org/10.3390/molecules24010154.

Sasadara, M., Nayaka, N., Yuda, P., Dewi, N., Cahyaningsih, E., Wirawan, I., & Silalahi, D. (2021). Optimization of chlorophyll extraction solvent of bulung sangu (Gracilaria sp.) seaweed. IOP Conference Series: Earth and Environmental Science.

Seyfoddin, A., & Al-Kassas, R. (2013). Development of solid lipid nanoparticles and nanostructured lipid carriers for improving ocular delivery of acyclovir. *Drug Development and Industrial Pharmacy, 39*(4), 508–519. https://doi.org/10.3109/03639045.2012.665460

Silva, K. A., Coelho, M. A. Z., Calado, V. M., & Rocha-Leão, M. H. (2013). Olive oil and lemon salad dressing microencapsulated by freeze-drying. *LWT-Food Science and Technology, 50*(2), 569–574. https://doi.org/10.1016/j.lwt.2012.08.005

Stefanescu, E. A. (2010). Influence of key parameters on the morphology of ethylcellulose microcapsules prepared via room-temperature spray drying. *Cellulose, 17*(3), 617–626. https://doi.org/10.1007/s10570-010-9399-5

Šturm, L., Črnivec, I. G. O., Istenič, K., Ota, A., Megušar, P., Slukan, A., Humar, M., Levic, S., Nedović, V., & Deželak, M. (2019). Encapsulation of non-dewaxed propolis by freeze-drying and spray-drying using gum Arabic, maltodextrin and inulin as coating materials. *Food and Bioproducts Processing, 116*, 196–211. https://doi.org/10.1016/j.fbp.2019.05.008

Tonon, R. V., Brabet, C., & Hubinger, M. D. (2010). Anthocyanin stability and antioxidant activity of spray-dried açaí (Euterpe oleracea Mart.) juice produced with different carrier agents. *Food Research International, 43*(3), 907–914.

Walton, D. (2000). The morphology of spray-dried particles a qualitative view. *Drying Technology, 18*(9), 1943–1986. https://doi.org/10.1080/07373930008917822

Wei, W. Y., & Periasamy, V. (2011). Synthesis, structural and spectroscopic properties of encapsulated Chlorophyll-a thin film in carboxymethyl cellulose. *Journal of Porphyrins and Phthalocyanines, 15*(02), 122–130. https://doi.org/10.1142/S1088424611003021

Zhang, B., Zheng, L., Liang, S., Lu, Y., Zheng, J., Zhang, G., Li, W., & Jiang, H. (2022). Encapsulation of capsaicin in whey protein and OSA-modified starch using spray-drying: Physicochemical properties and its stability. *Foods, 11*(4), 612. https://doi.org/10.3390/foods11040612

Zhang, H., Jiang, L., Tong, M., Lu, Y., Ouyang, X.-K., & Ling, J. (2021). Encapsulation of curcumin using fucoidan stabilized zein nanoparticles: Preparation, characterization, and in vitro release performance. *Journal of Molecular Liquids, 329*, Article 115586. https://doi.org/10.1016/j.molliq.2021.115586

Zhang, Z.-H., Peng, H., Ma, H., & Zeng, X.-A. (2019). Effect of inlet air drying temperatures on the physicochemical properties and antioxidant activity of whey protein isolate-kale leaves chlorophyll (WPI-CH) microcapsules. *Journal of Food Engineering, 245*, 149–156.

Zhang, Z.-H., Peng, H., Woo, M. W., Zeng, X.-A., Brennan, M., & Brennan, C. S. (2020). Preparation and characterization of whey protein isolate-chlorophyll microcapsules by spray drying: Effect of WPI ratios on the physicochemical and antioxidant properties. *Journal of Food Engineering, 267*, Article 109729.

Zhang, Z.-H., Wang, L.-H., Zeng, X.-A., Han, Z., & Wang, M.-S. (2017). Effect of pulsed electric fields (PEFs) on the pigments extracted from spinach (Spinacia oleracea L.). *Innovative Food Science & Emerging Technologies, 43*, 26–34. https://doi.org/10.1016/j.ifset.2017.06.014